Liquid Crystals
Publication details, including instructions for authors and subscription information:
http://www.informaworld.com/smpp/title~content=t713926090

Effects of the H-bond donor structure on the properties of supramolecular side chain liquid crystalline polymers based on poly(3-carboxypropylmethylsiloxane-*co*-dimethylsiloxane)s and stilbazoles

Xu Li; Suat Hong Goh Corresponding author; Yee Hing Lai

Online publication date: 21 May 2010

To cite this Article Li, Xu , Goh Corresponding author, Suat Hong and Lai, Yee Hing(2003) 'Effects of the H-bond donor structure on the properties of supramolecular side chain liquid crystalline polymers based on poly(3-carboxypropylmethylsiloxane-*co*-dimethylsiloxane)s and stilbazoles', Liquid Crystals, 30: 7, 811 — 821
To link to this Article: DOI: 10.1080/0267829031000121215
URL: http://dx.doi.org/10.1080/0267829031000121215

LIQUID CRYSTALS, VOL. 30, NO. 7, JULY, 2003, 811–821

Taylor & Francis
Taylor & Francis Group

Effects of the H-bond donor structure on the properties of supramolecular side chain liquid crystalline polymers based on poly(3-carboxypropylmethylsiloxane-*co*-dimethylsiloxane)s and stilbazoles

XU LI, SUAT HONG GOH* and YEE HING LAI
Department of Chemistry, National University of Singapore, 3 Science Drive 3, Singapore 117543

(*Received 9 September 2002; in final form 28 January 2003; accepted 26 February 2003*)

Supramolecular side chain liquid crystalline polymers (SCLCPs) based on poly(3-carboxypropylmethylsiloxane-*co*-dimethylsiloxane) (PSIX, X = 100, 76, 60, 41 or 23, denoting the mole percentage of 3-carboxypropylmethylsiloxane unit in the polymer) and stilbazole derivatives have been obtained through intermolecular hydrogen bonding (H-bonding) interactions between the carboxylic acid and the pyridyl moieties. The formation of H-bonding and self-assembly results in the formation of new mesogenic units, in which H-bonds function as molecular connectors. FTIR shows the existence of H-bonding in the complexes. The polymeric complexes behave as single component liquid crystalline polymers and exhibit stable and enantiotropic mesophases. The liquid crystalline properties of the supramolecular SCLCPs were studied using differential scanning calorimetry, polarizing optical microscopy and X-ray diffraction, and were found to exhibit smectic A phases with focal-conic textures. The thermal stability of the SCLCP increases on increasing the carboxylic acid content in the polysiloxane and the concentration of the stilbazole derivative in the complex. However, the thermal stability decreases on increasing the chain length of the stilbazole derivative. The crystal phase was not formed even on cooling to the glass transition temperature of the polymeric complex.

1. Introduction

In recent years side chain liquid crystalline polymers (SCLCPs), which combine properties characteristic of polymers with those of conventional low molar mass mesogens, have received much attention because of their potential importance in technological applications [1–12]. SCLCPs are generally prepared by covalently linking rigid mesogens to polymer backbones through flexible spacers. The function of the spacer is to decouple the motions of the polymer backbone from the self-ordering tendencies of the mesogens.

Instead of linking pendant mesogenic units covalently to the polymer backbone, self-assembly through specific interactions such as hydrogen bonding (H-bonding) [13–20], ionic [21–23], ion–dipole [24, 25] and charge transfer interactions [26, 27] has been recognized as a new strategy for constructing SCLCPs. Because of their simplicity of preparation, the self-assembled SCLCPs have the advantage of being able to fine-tune the liquid crystalline properties more readily. Various molecular parameters, such as the nature of the rigid core, the nature and the length of the terminal group, and the spacer length can be modified with relative ease, compared with covalently-bound systems. The H-bonding interaction is one of the most important and widely used non-covalent interactions. It may be located on or near the polymer backbone, or within the rigid mesogen. In the first case, the function of the H-bonding is just to attach the mesogenic unit to the polymer main chain leading to the formation of supramolecular SCLCPs. In the second case, the H-bonding not only attaches the mesogenic unit to the polymer main chain, it is also a component of the unit. Thus, the liquid crystalline properties can be tuned through selecting either the H-bond donor or acceptor. Upon the formation of H-bonding, a new mesogenic unit is obtained with a larger length to breadth ratio, yielding a thermally stable product with a high mesophase–isotropic transition temperature. Furthermore, the dynamics and the directionality of the H-bonding interaction can affect the properties of

*Author for correspondence; e-mail: chmgohsh@nus.edu.sg

Liquid Crystals ISSN 0267-8292 print/ISSN 1366-5855 online © 2003 Taylor & Francis Ltd
http://www.tandf.co.uk/journals
DOI: 10.1080/0267829031000121215

supramolecular SCLCPs by changing the shape of the mesogenic unit.

Fréchet *et al.* [13, 14] have reported the self-assembly of benzoic acid-containing polysiloxane and stilbazole derivatives. In their system, a novel mesogenic unit was formed through intermolecular H-bonding between the benzoic acid introduced as a pendant group on the polysiloxane backbone and the pyridyl ring in the stilbazole. The single H-bond between the H-bond donor and acceptor increased the length to breadth ratio of the H-bonded mesogenic unit, leading to a high smectic–isotropic phase transition temperature. Although the stability of the mesophase was increased, the thermal stability of the crystalline phase was also increased, and the mesomorphic temperature range decreased. However, in some cases, SCLCPs which exhibit mesogenic phases at relatively low temperatures are required. This is the very reason why polysiloxane is often selected as the backbone. When mesogenic groups are attached to the polysiloxane main chain, the low glass transition temperature (T_g) allows the liquid crystalline (LC) phase to form at a relatively low temperature [28–33].

In the present study, we have selected a series of carboxylic acid-containing polysiloxanes, specifically, poly(3-carboxypropylmethylsiloxane-*co*-dimethylsiloxane) (PSIX, X = 100, 76, 60, 41 or 23, denoting the mole percentage of 3-carboxypropylmethylsiloxane units in the polymer) as the H-bond donor polymer. The self-assembly of the stilbazole derivatives along the polysiloxane was studied by differential scanning calorimetry (DSC), polarizing optical microscopy (POM) and X-ray diffraction (XRD). As there is no conjugated benzene ring in the carboxylic acid group, it is possible that PSIX may exhibit different mesogenic properties compared with benzoic acid-containing polysiloxanes.

2. Experimental

2.1. *Materials*

(3-Cyanopropyl)methyldichlorosilane and dichlorodimethylsilane were supplied by Fluka Chemika-Biochemika Company. Poly(dimethylsiloxane) (PDMS) with a viscosity of 60 000 cSt, 4-hydroxybenzaldehyde, 4-picoline, acetic anhydride, bromoethane, 1-bromopropane, 1-bromobutane, 1-bromopentane, 1-bromohexane, 1-bromoheptane, 1-bromooctane and 1-bromodecane were supplied by Aldrich Chemical Co. All the chemicals were used as received. DMF was dried over molecular sieves (4 Å).

Table 1. Properties of the H-bond donor polymer. T_g = glass transition temperature; M_n = number-average molecular mass; M_w = weight-average molecular mass.

Polymer	T_g/°C	M_n/kg mol^{-1}	M_w/M$_n$
PSI23	−85	26	2.2
PSI41	−55	30	2.2
PSI60	−41	23	2.2
PSI76	−29	14	2.0
PSI100	−9	6.6	1.6

2.2. *Synthesis of carboxylic acid-containing polysiloxane*

The synthesis and characterization of PSIX compounds were reported previously [34]. The main properties of PSIX are summarized in table 1.

2.3. *Synthesis of trans-4-alkoxy-4′-stilbazoles*

trans-4-Hydroxy-4′-stilbazole was synthesized following the procedures of Kumar *et al* [13]. Eight *trans*-4-alkoxy-4′-stilbazoles were prepared by reacting *trans*-4-hydroxy-4′-stilbazole with either bromoethane, 1-bromopropane, 1-bromobutane, 1-bromopentane, 1-bromohexane, 1-bromoheptane, 1-bromooctane or 1-bromodecane. A typical synthetic procedure for *trans*-4-butoxy-4′-stilbazole is given:

trans-4-Hydroxy-4′-stilbazole (7.25 g, 36.80 mmol) was dissolved in 125 ml DMF under N_2, followed by addition of 10.45 g (75.72 mmol) K_2CO_3, and stirred for 0.5 h at room temperature. Then, 4.89 g (35.70 mmol) of 1-bromobutane was added. After the reaction had proceeded at room temperature for 36 h, DMF was removed and the product extracted with $CHCl_3$. The $CHCl_3$ layer was washed first with 5% NaOH aqueous solution 3 times, and then repeatedly with water to neutral pH. Purification was done by flash silica gel column chromatography using dichloromethane/methanol (30/1) as eluant to give the desired product. ^{1}H NMR ($CDCl_3$, ppm): 8.54, 7.33 (pyridyl), 7.47, 6.91 (phenyl), 7.25, 6.85 (CH–CH), 4.00 (OCH_2), 1.81 ($OCCH_2$), 1.50 ($OCCCH_2$), 1.00 (CH_3). Anal: calcd for $C_{17}H_{19}ON$, C 80.63, H 7.51, N 5.53; found, C 80.28, H 7.94, N 5.12%.

2.4. *Preparation of hydrogen-bonded complexes*

All hydrogen-bonded complexes were prepared by solution casting using tetrahydrofuran (THF) as solvent. Complete removal of THF was ensured by slow evaporation at room temperature initially and followed by drying *in vacuo* for 2 weeks at 60°C. Unless otherwise stated, the complex contains an equimolar ratio of carboxylic acid and pyridine groups.

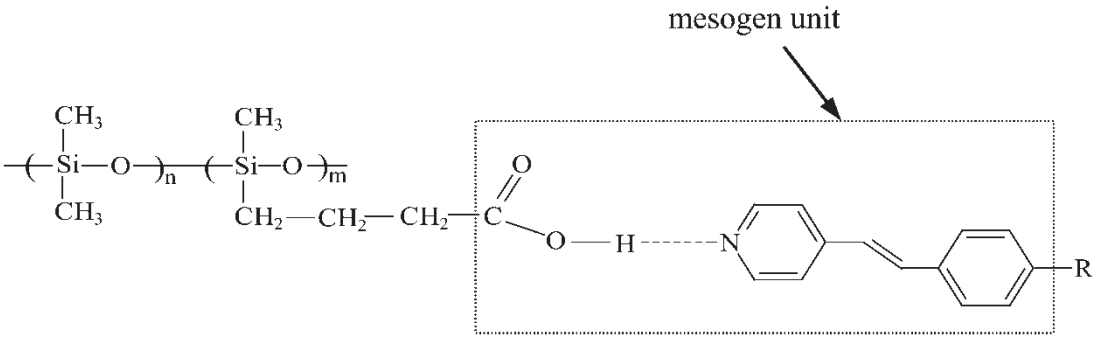

2.5. *Characterization*

Nuclear magnetic resonance (NMR) spectra were recorded on a Bruker ACF 300 spectrometer at 25°C with TMS as an internal standard. FTIR spectra were recorded on a Bio-Rad 165 FTIR spectrophotometer; 64 scans were signal-averaged with a resolution of $2\,cm^{-1}$. Samples were prepared by dispersing the complexes in KBr and compressing the mixtures to form disks. Spectra were recorded at a specific temperature, using a SPECAC high temperature cell equipped with an automatic temperature controller, which was mounted in the spectrophotometer.

DSC measurements were performed on a TA Instruments 2920 differential scanning calorimeter equipped with an auto-cool accessory and calibrated using indium. The following protocol was used for each sample: heating from room temperature to 150°C at $20^{\circ}C\,min^{-1}$, isothermally held at 150°C for 3 min, cooling from 150 to −20°C at $10^{\circ}C\,min^{-1}$ and finally re-heating from −20 to 150°C at $10^{\circ}C\,min^{-1}$. Data were collected during the second heating run to isotropic state and the first cooling run from the isotropic state. Transition temperatures were taken as the maxima of the peaks.

The mesophase textures exhibited by the complexes and the stilbazoles were observed under an Olympus BX50 polarizing optical microscope (magnification 400×) equipped with a Linkam THMS-600 hotstage which was controlled by a central processor. The software used in the processing of images is Image-pro plus 3.0. The sample was pressed between a glass slide and a cover slip and observed in the LC phase. The heating/cooling rate was $2^{\circ}C\,min^{-1}$.

XRD measurements were carried out on a Siemens D5005 Diffractometer (40 kV, 30 mA) using Ni-filtered CuK_{α} radiation in 0.01° steps from 1.5° to 27° (in 2θ) with 1 s per step. The intensity of the diffracted X-rays from the samples was measured by a scintillation counter. The samples were annealed by heating to their isotropization temperatures followed by gradually cooling to room temperature prior to XRD studies. Bragg's equation was used to calculate the layer spacings of the various reflections.

3. Results and discussions

3.1. *Formation of hydrogen-bonded side chain liquid crystalline polymers*

The self-assembly process between the H-bond donor PSIX and the monofunctional H-bond acceptors ST*n* is shown in the scheme:

PSI100, $m=1.00$; PSI76, $m=0.76$; PSI60, $m=0.60$; PSI41, $m=0.41$; PSI23, $m=0.23$. $(m+n=1.00)$

ST0, $R=H$; ST2, $R=OCH_2CH_3$; ST3, $R=OCH_2CH_2CH_3$; ST4, $R=OCH_2(CH_2)_2CH_3$; ST5, $R=OCH_2(CH_2)_3CH_3$; ST6, $R=OCH_2(CH_2)_4CH_3$; ST7, $R=OCH_2(CH_2)_5CH_3$; ST8, $R=OCH_2(CH_2)_6CH_3$; ST10, $R=OCH_2(CH_2)_8CH_3$.

The thermal behaviour of the stilbazoles and their complexes with PSIX was studied by DSC. Figure 1 shows the DSC curves of ST4 and its complexes with polydimethylsiloxane (PDMS) or PSI100, and the transition temperatures and the associated enthaply changes, ΔH, are listed in table 2. Curve (*a*) shows the first cooling run for ST4. An exothermic peak is seen at 83°C with an enthalpy change of $17.96\,kJ\,mol^{-1}$. A POM study shows that the exothermic peak arises from the transition from the isotropic to crystalline state. The XRD pattern of ST4, which will be discussed in a later section, also confirms the formation of a crystal below 83°C. Curve (*a*′) shows the second heating run for ST4. Two overlapping endothermic peaks around 93°C are observed which are identified as the melting of the crystal on the basis of visual observation and XRD measurements. The appearance of two overlapping endothermic peaks is due to the coexistence of two types of crystal phase. The PDMS/ST4 complex shows a similar phase transition to that of pure ST4, figure 1 curves (*b*) and (*b*′). On heating, only one endothermic peak due to the crystal–isotropic liquid transition is observed at 83°C. The enthalpy change of the transition

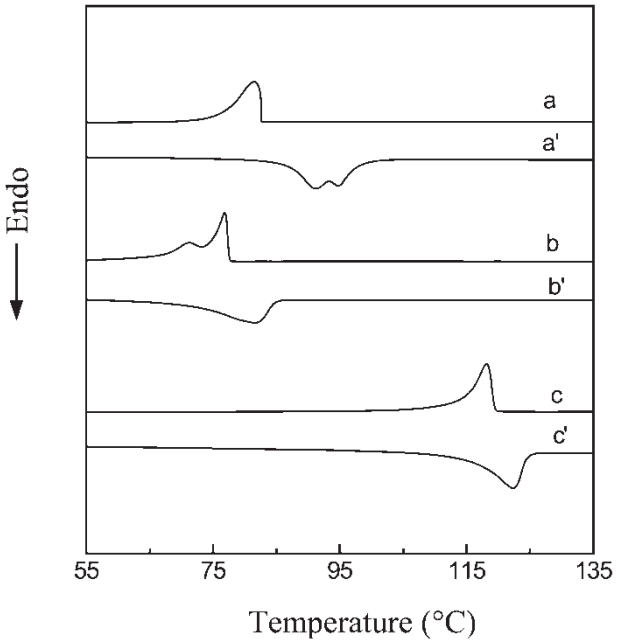

Figure 1. DSC curves of ST4 and its complexes with PDMS or PSI100. First cooling run: (*a*) ST4, (*b*) PDMS/ST4, (*c*) PSI100/ST4. Second heating run: (*a'*) ST4, (*b'*) PDMS/ST4, (*c'*) PSI100/ST4.

Table 2. Transition temperatures (°C) and associated enthalpy changes (kJ mol^{-1}, in parentheses) of ST4 and its complexes. I = isotropic phase; Cr = crystalline phase; SmA = smectic A phase; g = glassy phase.

Sample	1st cooling	2nd heating
ST4	I 83(17.96) Cr	Cr_1 88(6.6) Cr_2 93(8.37) I
PDMS/ST4	I 77(14.58) Cr_1 71(4.19) Cr_2	Cr 83(15.79) I
PSI100/ST4	I 118(18.04) SmA	G 12 SmA 122(19.01) I

is 15.79 kJ mol^{-1}. On cooling, there are two overlapping peaks at 77 and 71°C with enthalpy changes of 14.58 and 4.19 kJ mol^{-1}, respectively. The transition temperatures are lower than that of pure ST4. The lower transition temperatures are due to the diluting effect of PDMS on the ordering in the crystal. The complex showed no birefringent behaviour when examined by POM.

Curves (*c*) and (*c'*) are DSC curves for the PSI100/ST4 complex. The phase transition temperatures of the complex are higher than those of pure ST4 and the PDMS/ST4 complex. There is one exothermic peak at 118°C with an enthalpy change of 18.04 kJ mol^{-1} in the first cooling process, corresponding to the transition from the isotropic phase to a liquid crystalline phase, curve (*c*). An endothermic peak is observed in the second heating run due to the transition from the liquid crystalline phase to the isotropic state at 122°C with an enthalpy change of 19.01 kJ mol^{-1}. POM observations and XRD measurements (which will be discussed in a later section) show that the phase transition is between the isotropic phase and the smectic A phase. The breadth of the smectic–isotropic transition is likely to be due to the polydisperse nature of the polymers in these complexes. Thus, the complex prepared from two different non-mesogenic components behaves as a single mesogenic compound.

The existence of intermolecular H-bonding in the supramolecular SCLCPs is confirmed by FTIR measurements. Figure 2 shows the FTIR spectra of PSI100, ST4 and their complexes of varying composition. PSI100 exhibits a satellite band around 2620 cm^{-1} attributed to dimeric carboxylic acid groups as commonly observed in other carboxylic acids [35–38]. Upon mixing PSI100 with ST4, the satellite band (2620 cm^{-1}) shifts towards a lower wave number and a new broad band centered around 1920 cm^{-1} appears. With increasing ST4 content in the complex, the extent of the shift of the satellite band increases and the weak broad band becomes more distinct. PSI100 exhibits a rather broad carbonyl stretching band at around

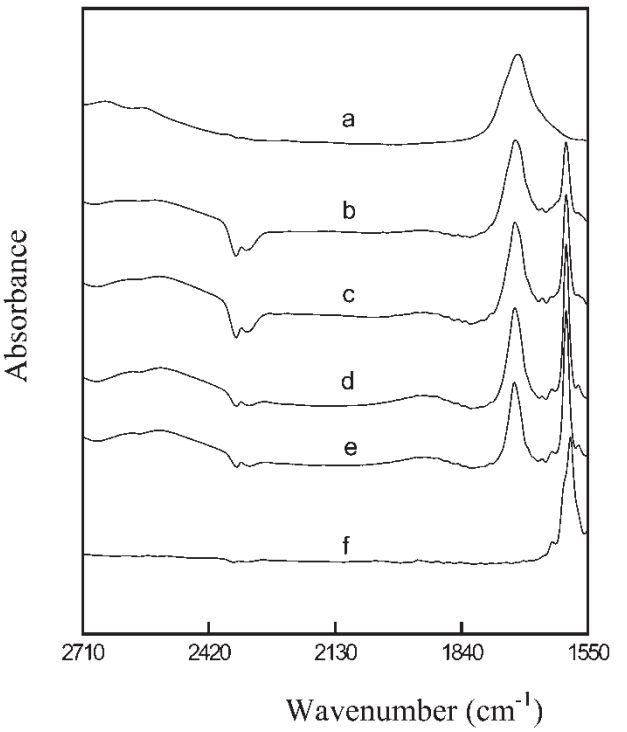

Figure 2. FTIR spectra of PSI100, ST4 and their complexes having different ratios. (*a*) PSI100; (*b*) PSI100/ST4 (1:0.4); (*c*) PSI100/ST4 (1:0.6); (*d*) PSI100/ST4 (1:0.8); (*e*) PSI100/ST4 (1:1); (*f*) ST4.

1710 cm^{-1} consisting of two overlapping carbonyl stretching modes associated with free and self-associated carboxylic acid groups curve (*a*) in figure 2. The latter is at a lower wave number than the former.

In the PSI100/ST4 complexes, the carbonyl stretching band narrows sharply with the band centre moving to 1721 cm^{-1}. These changes are consistent with the liberation of carbonyl groups from the carboxylic acid dimer when PSI100 interacts with ST4. The characteristic pyridine vibrational modes also show changes upon mixing PSI100 with ST4. As shown in figure 2, ST4 exhibits a pyridine ring band at 1590 cm^{-1}. However, this band shifts slightly to a higher wave number with increasing PSI100 content in the complex, resulting from an increase in the rigidity of the pyridine ring due to intermolecular interaction. All these are indications of strong H-bonding between the carboxylic acid of PSI100 and the pyridyl ring in ST4. Similar results were also observed in PSIX/poly(vinylpyridine) blends [34].

The high value of the enthalpy change seen for the PSI100/ST4 complex is attributed to the dissociation of the H-bonding at the smectic–isotropic transition. In the highly ordered smectic phase, H-bonding is more stable than in the isotropic state, due to co-operation between the mesogenic units. The isotropization of the smectic phase accelerates dissociation of the H-bonding. This is confirmed by FTIR measurements of the PSI100/ST4 complex at different temperatures. As discussed already the shift of the satellite peak at 2620 cm^{-1} in PSI100 to a lower wave number region, and the appearance of a broad peak at 1920 cm^{-1}, indicate the formation of H-bonding between the carboxylic acid groups in PSI100 and the pyridyl rings in ST4. As shown in figure 3, as the temperature was increased from 25 to 160°C, the extent of the frequency shift of the satellite peak and the intensity of the broad peak at 1920 cm^{-1} decreased. A shoulder at 1738 cm^{-1} of the carbonyl band at around 1721 cm^{-1} is also observed in figure 3 when the temperature is 140°C or above. At 160°C, the broad peak at 1920 cm^{-1} disappeared after 2 h. However, after cooling to room temperature, the broad peak reappeared with almost the same intensity as originally. The apparent shape change of the carbonyl band from 105 to 140°C, as well as the significant decrease of the frequency shift and the intensity, is due to the dissociation of the H-bonding corresponding to the isotropization of the smectic A phase at around 122°C. Similar temperature effects on hydrogen bonding stability has previously been observed in other pyridyl-carboxylic acid systems [39–41]. It is of interest to note the pronounced reduction in the intensity of the band at *c*. 1600 cm^{-1} after annealing

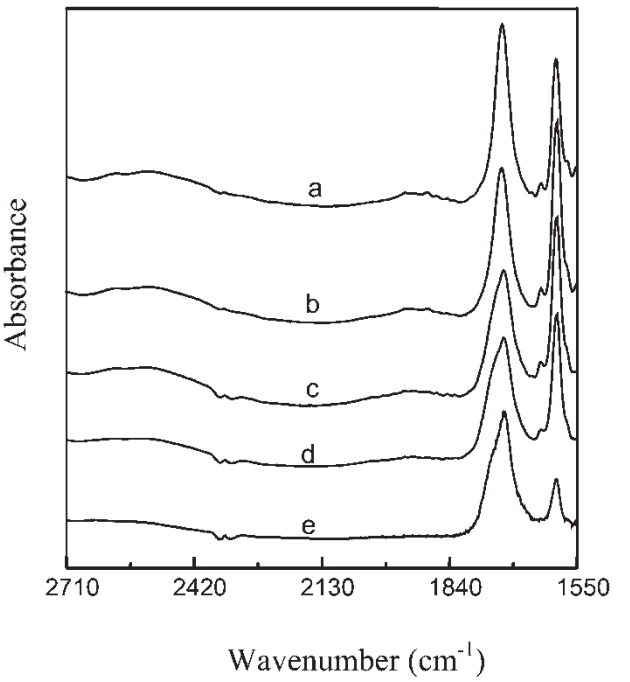

Figure 3. FTIR spectra of the PSI100/ST4 complex (1:1) at different temperatures. (*a*) 80°C; (*b*) 105°C; (*c*) 140°C; (*d*) 160°C; (*e*) 160°C; for 2h.

at 160°C for 2 h. This could arise from the disruption of the preferential orientation of the pyridine ring under prolonged heat treatment.

3.2. *Effect of the H-bonding structure*

Fréchet *et al.* [13, 14] have reported the formation and properties of supramolecular liquid crystals formed from a series of benzoic acid-containing polysiloxanes and some stilbazole derivatives. They found that the H-bonding between the benzoic acid and the stilbazole not only attached the stilbazole unit to the polysiloxane, but also increased the length to breadth ratio of the mesogenic unit. As a result, the stability of the liquid crystal phase increased. At the same time, however the stability of the crystal also increased. They observed that the melting point of the crystalline phase was around 90°C. For the complexes we prepared from carboxylic acid-containing polysiloxanes and stilbazole derivatives, crystallinity was not observed, not even on cooling to T_g (T_g = 12°C for PSI100/ST4 complex) at 1°C min^{-1}; the sample remained unchanged in the smectic state.

In the stilbazole derivatives, due to the polarization effect of the N atom on the C–H bond in the α position of the pyridine ring, there exists a weak $C–H_\alpha$—O interaction. Such an interaction plays an important role on the formation of crystal and supramolecules and

affects their conformations [42, 43]. Although weak, it is sufficient to select a particular crystallization pathway from among several possibilities. Upon formation of the N—H–O H-bond and the weak C–H_{α}—O interaction, the complexes formed by pyridine ring and carboxylic acid group are more likely to adopt a coplanar geometry which facilitates the formation of the crystalline phase and the higher order mesogenic phases. The optimized binding geometry at the HF/6-31 G* level of the complexes formed by a pyridine ring and carboxylic acid group is shown below [44].

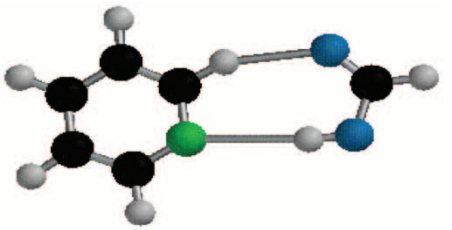

When the stilbazole and benzoic acid groups are arranged in the binding pattern shown above, the idealized geometry of the core of the complex is as shown below.

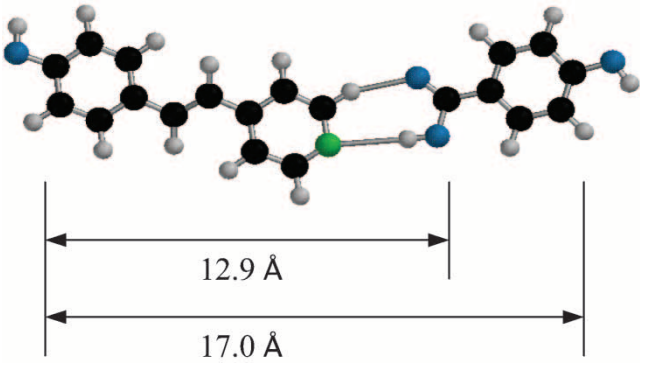

While the length to breadth ratio is 2.6 for the stilbazole derivative the ratio for the core is 4.1. However, when the carboxylic acid group is used, the length to breadth ratio is only 3.1. Therefore, when a carboxylic acid is used instead of benzoic acid, the increase in the length to breadth ratio is limited. Even though H-bonding in the complexes can attach stibazole to the polysiloxane backbone, leading to the formation of a liquid crystalline phase, the smaller increase of the length to breadth ratio does not lead to the formation of crystalline phases, which makes it possible to obtain liquid crystalline behaviour near room temperature. Thus, through selecting different H-bond donor groups, the properties of supramolecular SCLCPs can be adjusted.

3.3. *Effects of the composition of complexes, the carboxylic acid content in PSIX and the tail length of stilbazole*

To ascertain how composition affects the mesomorphic properties of these supramolecular assembles, a number of PSI100/ST4 complexes of varying composition were prepared. These complexes are miscible over the whole composition range when observed using POM. The DSC curves of the first cooling run and second heating run of various complexes are shown in figures 4 and 5, respectively. The transition temperatures and the associated enthalpy changes of the complexes are shown in table 3. With increasing concentration of ST4, the isotropization temperature and the associated enthalpy change initially increase until the PSI100/ST4 ratio reaches 1:1, and then decrease with further increase of the ratio. This composition-dependent thermal stability of the polymeric liquid crystalline phase may be attributed to the higher degree of cooperative intermolecular interaction and to the paired mesogen effect at higher concentrations of the hydrogen-bonded species. The formation of such supramolecular LCs is due to the attachment of low molecular mass compounds along the polymer backbone through H-bonding between the carboxylic acid groups in PSI100 and the pyridyl rings in ST4. When the PSI100/ST4 ratio is below 1:1, the higher the concentration of ST4, the higher the concentration of the hydrogen-bonded mesogenic units. Thus, the thermal

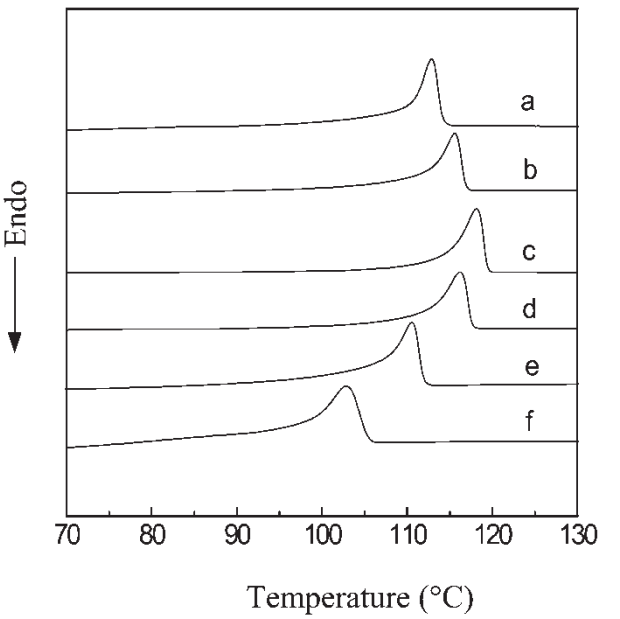

Figure 4. DSC curves of the PSI100/ST4 complexes with differing molar ratios. First cooling run: (*a*) 1:1.4; (*b*) 1:1.2; (*c*) 1:1; (*d*) 1:0.8; (*e*) 1:0.6; (*f*) 1:0.4.

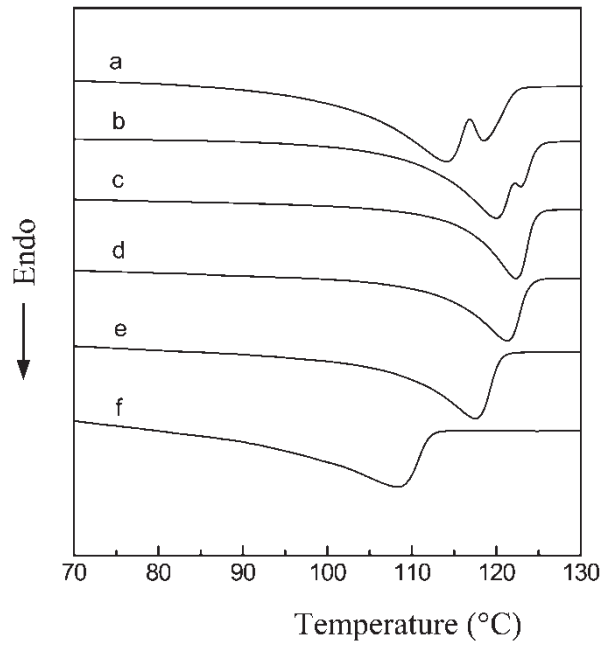

Figure 5. DSC curves of the PSI100/ST4 complexes with differing molar ratios. Second heating run (*a*) 1:1.4; (*b*) 1:1.2; (*c*) 1:1; (*d*) 1:0.8; (*e*) 1:0.6; (*f*) 1:0.4.

stability of the liquid crystalline phase increases with increasing concentration of ST4 in the PSI100/ST4 complex. On the other hand, although a spacer helps to decouple the mesogenic units from the main chain, decoupling is nevertheless incomplete. The connection of the mesogenic unit to the polymer backbone increases the rigidity of the polymer backbone, and restricts the motions of the mesogenic units, facilitating the packing of the mesogenic units along a specific direction. As a result, the clearing temperature of the mesophase increases with increasing feed ratio of ST4 to carboxylic acid. The increase in the rigidity of the polymer backbone is shown by the change of T_g from -2°C at a molar ratio of 0.4 to 12°C at a molar ratio of 1.0.

When the molar ratio of PSI100 to ST4 is 1:1.2 or higher, there are insufficient carboxylic acid groups available to interact with ST4 in a 1:1 ratio. As a result, some ST4 cannot be associated with the polymer backbone through H-bonding. Although they may be incorporated into a LC phase with similar smectic A textures through intermolecular interactions between the low molecular mass compounds, the alignment order of the phase is lower. Consequently, the transition temperatures and enthalpy changes decrease when this ratio is higher than 1:1. This is confirmed by the appearance of two overlapping endothermic peaks in the second heating DSC curve, indicating the coexistence of two kinds of smectic A phases SmA_1 and SmA_2 or two domains.

Table 4. Transition temperatures (°C) and associated enthalpy changes (kJ mol^{-1}, in parentheses) of PSIX/ST4 complexes (1:1) with differing carboxylic acid contents in PSIX. I = isotropic phase; SmA = smectic A phase; g = glassy phase.

Complex	1st cooling	2nd heating
PSI100/ST4	I 118(18.04) SmA	g 12 SmA 122(19.01) I
PSI76/ST4	I 108(15.92) SmA	g −3 SmA 115(17.93) I
PSI60/ST4	I 102(11.69) SmA	g −9 SmA 110(13.79) I
PSI41/ST4	I 99(7.05) SmA	g −17 SmA 105(9.68) I

The thermal properties of PSIX/ST4 complexes having a 1:1 stoichiometry of the carboxylic acid groups and stilbazole ST4 units are given in table 4. The supramolecular 'homopolymer' may be considered as a copolymer polymerized from the mesogenic monomer of the hydrogen-bonded ST4 and non-mesogenic monomer. On increasing the carboxylic acid content in PSIX, the mesogenic unit in the 'copolymer' increases, and the stability of the LC increases. As shown in table 4, the phase transition temperatures and enthalpy changes increase from 99°C and 7.05 kJ mol^{-1} for the PSI41/ST4 complex to 118°C and 18.04 kJ mol^{-1} for the PSI100/ST4 complex in the cooling run. This reflects the increase of the number of mesogenic units attached to the polymer backbone.

For SCLCPs, the terminal group of the mesogenic unit plays an important role on phase behaviours. The chain length was found to influence critically the mesophase characteristics of the polymers [29, 45]. A plot of the transition temperatures as a function of the

Table 3. Transition temperatures (°C) and associated enthalpy changes (kJ mol^{-1}, in parentheses) of PSI100/ST4 complexes having differing molar ratios. I = isotropic phase; SmA = smectic A phase; g = glassy phase.

Complex	1st cooling	2nd heating
PSI100/ST4 (1:1.4)	I 111(16.01) SmA	g 12 SmA_1 114(2.66) SmA_2 119(1.09) I
PSI100/ST4 (1:1.2)	I 116(16.25) SmA	g 14 SmA_1 120(3.27) SmA_2 123(0.06) I
PSI100/ST4 (1:1)	I 118(18.04) SmA	g 12 SmA 122(19.01) I
PSI100/ST4 (1:0.8)	I 116(9.59) SmA	g 9 SmA 121(9.06) I
PSI100/ST4 (1:0.6)	I 113(5.57) SmA	g 5 SmA 118(5.89) I
PSI100/ST4 (1:0.4)	I 103(2.56) SmA	g −2 SmA 109(2.60) I

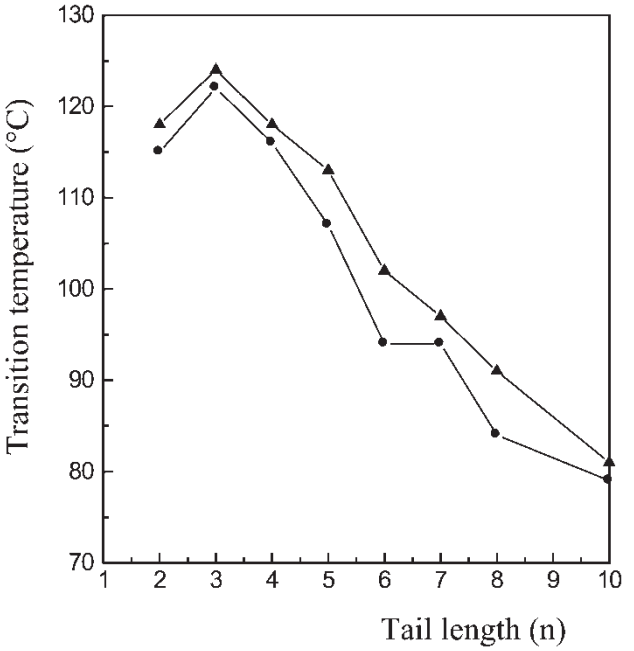

Figure 6. Dependence of the transition temperatures of PSI100/ST*n* complexes on the chain length *n* in the stilbazole unit on cooling (▲) PSI100/ST*n* (1:1) and (●) PSI100/ST*n* (1:0.8).

alkyl chain length *n* of the stilbazole unit in the cooling run is shown in figure 6. When the stilbazole ST0 was used as the mesogenic unit, the complex PSI100/ST0 showed no liquid crystalline behaviours over the whole temperature range examined. The isotropic–smectic transition temperature of the complexes increases from 118°C for the PSI100/ST2 complex to 124°C for the PSI100/ST3 complex when the feed ratio is 1:1, and from 115°C for the PSI100/ST2 complex to 122°C for the PSI100/ST3 complex when the feed ratio is 1:0.8. An increase in the enthalpy change is also observed, and the data are shown in table 5. Generally, the thermal stability of the liquid crystalline phase of SCLCPs is dependent on the length to breadth ratio of the mesogenic unit as discussed earlier. The larger the ratio, the better the thermal stability. When the terminal group is changed from H to OCH_2CH_3 and to $OCH_2CH_2CH_3$, the increase of its length leads to an increase of the length to breadth ratio, thereby enhancing the thermal stability of the SCLCPs. However, when the stilbazole ST4 or others with longer tail length are used as mesogenic units, the isotropic–smectic temperature decreases on increasing the tail length (figure 6 and table 5). The isotropic–smectic temperature decreases from 124°C for the PSI100/ST3 complex to 81°C for the PSI100/ST10 complex when the feed ratio is 1:1, and from 122°C for the PSI100/ST3 complex to 78°C for the PSI100/ST10 complex when the feed ratio is 1:0.8. It is well known that alkyl and related groups are flexible, due to the relatively low energy barrier necessary for the change from the *trans* to the *gauche* conformation. There is a mixture of all possible conformations in a temperature-dependent equilibrium. At a higher temperature the amount of *gauche* conformers will be larger than at a lower temperature, and the anisotropy of the alkyl chain is reduced. In the present study, the amount of *gauche* conformers increases with increasing tail length and the anisotropy of the alkyl chain is thus reduced. As a result, the isotropic–smectic transition temperature decreases with increasing tail length.

3.4. *Textures of the hydrogen-bonded side chain liquid crystalline polymer*

To confirm further the mesomorphic nature of these assembles and identify their textures, hot stage polarizing optical microscopy (POM) was employed. For the microscopic study all the samples were cooled from their isotropization temperatures at $2^{\circ}C\,min^{-1}$ prior to analysis. Figure 7 shows typical POM photographs of the PSI100/ST4 complex (1:1) observed in the LC phase on cooling. Thus, on from the isotropic phase, the formation of bâtonnets was observed initially. As the temperature gradually decreased, these bâtonnets eventually formed a focal-conic fan texture, characteristic of the smectic A phase; no

Table 5. Transition temperatures (°C) and associated enthalpy changes ($kJ\,mol^{-1}$, in parentheses) of PSI100/ST*n* complexes (1:1) with differing chain lengths on the stilbazole. I = isotropic phase; SmA = smectic A phase.

Complex	PSI100/ST*n* (1:1) 1st cooling	PSI100/ST*n* (1:0.8) 1st cooling
PSI100/ST2	I 118(11.25) SmA	I 115(7.62) SmA
PSI100/ST3	I 124(14.62) SmA	I 122(10.08) SmA
PSI100/ST4	I 118(18.04) SmA	I 116(9.59) SmA
PSI100/ST5	I 113(12.12) SmA	I 107(7.39) SmA
PSI100/ST6	I 102(6.10) SmA	I 94(5.56) SmA
PSI100/ST7	I 97(10.71) SmA	I 94(7.30) SmA
PSI100/ST8	I 91(11.00) SmA	I 84(5.04) SmA
PSI100/ST10	I 81(11.41) SmA	I 78(4.89) SmA

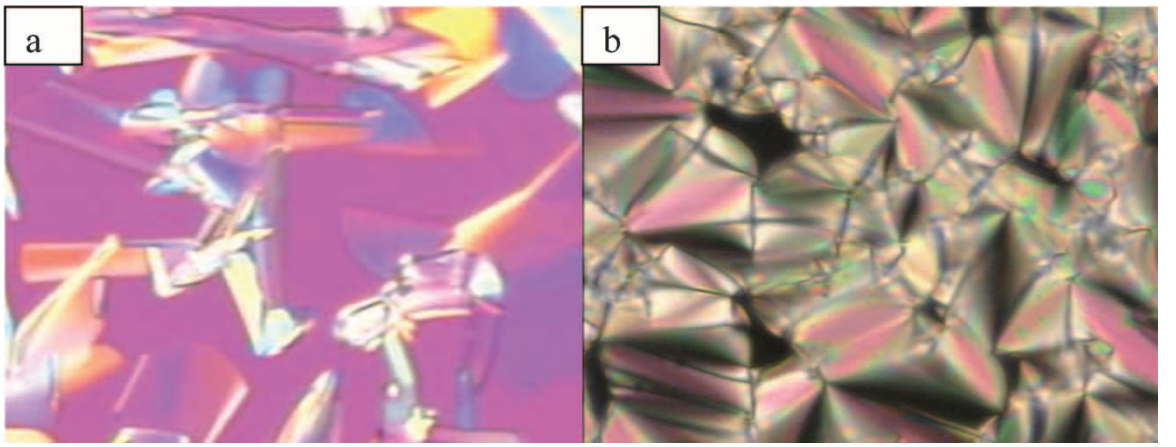

Figure 7. Optical micrographs of the PSI100/ST4 complex (1:1). (*a*) bâtonnets and (*b*) focal-conical texture at 96°C (400X).

further change of the texture was observed. The same phenomenon was observed for the other complexes. Therefore, the mesophases of these complexes are assigned as smectic A, which is further confirmed by XRD as discussed in the following section.

3.5. *X-ray diffraction studies on mesomorphic properties*

Figure 8 shows the flat film XRD patterns at 25°C for ST4 and its complexes with PSIX (PSIX/ST4) which had been cooled gradually from the isotropic phase. At room temperature, the X-ray pattern of ST4 exhibits several sharp diffractions in the angle range 1.5° to 27° (curve a). The low angle reflections indicate a layer-like structure and the high angle reflections indicate an ordered structure within the layer characteristic of a crystalline structure. For ST4, a sharp first order reflection at $2\theta = 5.7°$ corresponding to 15.4 Å was observed. Molecular modelling using standard bond lengths and bond angles for ST4 with the methylene units in their fully extended conformation gives a length of 14.5 Å from the pyridyl with N to the group in the alkoxy chain of ST4. Compared with the measured layer length in the XRD measurement, this indicates that the layer-like structure of the crystal is composed of a monolayer of ST4 in its fully extended conformation. The sharp peak at $2\theta = 11.4°$ corresponding to 7.8 Å and that at 17° corresponding to 5.2 Å can be regarded as the second and third order reflections of the first order reflection at $2\theta = 5.7°$, respectively. The sharp peaks in the wide angle region are due to intermolecular spacing. The XRD pattern of ST4 at room temperature indicates a crystal phase. On the other hand, in the pattern (curve f) of the PSI100/ST4 complex, there are two sharp but weak reflections at $2\theta = 3.4°$ and 10.6° in the small angle region, and two broad but strong peaks at $2\theta = 20.5°$ and 22.6° in the wide angle region at room temperature. The sharp peak at $2\theta = 3.4°$ corresponding to 26.2 Å can be regarded as the thickness of the smectic layer, while the reflection peak at $2\theta = 10.6°$ corresponding to 8.3 Å is due to the third order reflection of the smectic layer. The two broad reflections at $2\theta = 20.5°$ and 22.6° correspond to intermolecular spacings of 4.3 and 3.9 Å, which are indicative of a smectic mesophase.

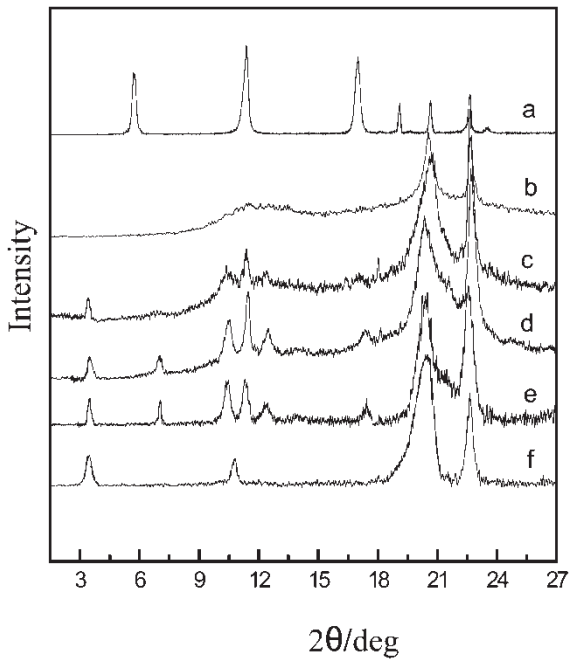

Figure 8. X-ray diffraction patterns of ST4 and PSIX/ST4 complexes at 25°C. (*a*) ST4; (*b*) PSI20/ST4; (*c*) PSI41/ST4; (*d*) PSI60/ST4; (*e*) PSI76/ST4; (*f*) PSI100/ST4.

Unlike a covalent bond, the length of a H-bond may vary under different conditions. For a H-bond between a pyridyl nitrogen and a carboxylic acid hydrogen, the

length can vary from 1.72 to 1.76 Å [46]; we chose 1.74 Å as an approximation. The bond angle of the H-bond is known to vary between 152° and 177° [46], and an average bond angle of 167° was used. It is well known that the polysiloxane backbone is confined between the smectic layers in SCLCPs [44]; the mesogenic length should then be equal to the length of the side chain. Molecular modelling using standard bond lengths and bond angles of the low molecular mass analogue of the PSI100/ST4 complex, with the methylene units in their fully extended conformation, gives a mesogenic length of 21.1 Å from the end of the methyl group in the alkoxy group of ST4 to the backbone of PSI100. The layer spacing of 26.2 Å being substantially less than twice the mesogen length, but greater than the mesogenic length, suggests a smectic A phase in which the side chains overlap:

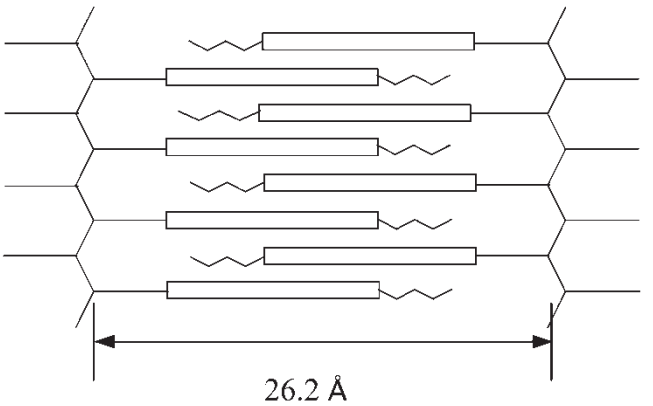

In the ST4/PSI100 complexes, PSI100 recognizes and binds the ST4 components along its backbones and self-assembles into a layered structure, giving to the smectic A texture. Due to the dipolar interactions between mesogenic units, the side chains overlap in the smectic A phase.

The carboxylic acid content in PSIX affects the structure of the smectic phase of the complexes. In figure 8, curves b–f show the XRD patterns of PSI23/ST4, PSI41/ST4, PSI60/ST4, PSI76/ST4 and PSI100/ST4 complexes, respectively. The carboxylic acid content in PSI23 is so small that in the PSI23/ST4 complexes the smectic phase cannot form. As shown in curve b, there is no sharp reflection in the small angle region at around $2\theta = 3.4°$ in the XRD pattern of the PSI23/ST4 complex. When the carboxylic acid content is 41% or above, a sharp reflection peak at around $2\theta = 3.4°$ appears and its relative intensity increases on increasing the carboxylic acid content in PSIX. This means that 41% of hydrogen-bonded mesogenic stilbazole units in the superamolecular SCLPCs is sufficient for the formation of the smectic layer. But, the two broad peaks at $2\theta = 20.5°$ and 22.6°, corresponding to intermolecular spacings of 4.3 and 3.9 Å, remained around the same positions for all the PSIX/ST4 complexes. This is in agreement with the expectation that for the same mesogenic units the same intermolecular arrangements in the complexes would be observed.

A reflection at around 6.9°, corresponding to 12.7 Å, i.e. the second order reflection of the first order reflection at $2\theta = 3.4°$, should appear in all the XRD patterns of these complexes. In fact, it only appears in the patterns of the PSI76/ST4 and PSI60/ST4 complexes. This is because some structural regularity interferes with the appearance of the second order reflection. There is a broad reflection at 11.3° corresponding to 7.8 Å in the XRD patterns of these complexes except for that of PSI100/ST4. In PSI23, PSI41, PSI60 and PSI76, there are some non-mesogenic dimethylsiloxane backbone moieties. After these PSIX samples were mixed with ST4, the complexes obtained can be regarded as copolymers containing mesogenic and non-mesogenic units. The non-mesogenic units may aggregate to form a non-mesogenic phase of size about 7.8 Å. On the other hand, the PSI100/ST4 complex is equivalent to a homopolymer, and therefore such a non-mesogenic phase is not present.

Table 6 shows the largest *d* spacing seen for the PSI100/ST4, PSI100/ST6, PSI100/ST8 and PSI100/ST10 complexes of equal molar ratio. The first order, sharp reflection corresponding to the layer spacing shifts to the small angle region on increasing the chain length of the stilbazole. The corresponding layer spacing of the complex increases from 26.2 Å for the PSI100/ST4 complex to 36.2 Å for the PSI100/ST10 complex, indicating that the alkyl chains in the stilbazole are in an extended conformation. The difference between the layer spacing lengths of two neighbouring complexes in the series increases with increasing stilbazole chain length, indicating that the degree of overlap decreases. Normally, the overlap is due to the interaction between two nearby mesogenic units. On increasing chain length, the concentration of the mesogenic units in the complex decreases, which leads to a decrease in the mesogenic unit interactions. As a result, the intensity of the overlap is decreased.

Table 6. The largest *d* spacing (Å) of the smectic A phase in PSI100/ST*n* complexes (1:1).

PSI100/ST*n* complex	*d* spacing
PSI100/ST4	26.2
PSI100/ST6	27.3
PSI100/ST8	28.6
PSI100/ST10	32.6

4. Conclusion

Supramolecular side chain liquid crystalline polymers have been built through hydrogen bonding between the carboxylic acid groups in a polysiloxane and the pyridyl ring in stilbazoles. The thermal transition temperatures, mesomorphic properties and mesophase textures of the polymeric complexes were characterized via a combination of DSC, POM and XRD. Unlike SCLCPs based on benzoic acid-containing polysiloxanes and stilbazoles, the PSIX/stilbazole SCLCPs do not exhibit crystallinity. The thermal stability of each complex is dependent on the carboxylic acid content in the polysiloxane, the composition of the complex and the chain length of the stilbazole. POM and XRD results indicate that the polymeric complexes exhibit a smectic A phase.

References

[1] Imrie, C. T., Karasz, F. E., and Attard, G. S., 1994, *Macromolecules*, **27,** 1578.
[2] Chen, Y., Harrison, W. T. A., Imrie, C. T., and Ryder, K. S., 2002, *J. mater. Chem.*, **12,** 579.
[3] Chen, Y., Imrie, C. T., and Ryder, K. S., 2001, *J. mater, Chem.*, **11,** 990.
[4] Stewart, D., Machattie, G. S., and Imrie, C. T., 1998, *J. mater. Chem.*, **8,** 47.
[5] Imrie, C. T., and Craig, A. A., 1999, *Macromolecules*, **32,** 6215.
[6] Imrie, C. T., Ingram, M. D., and Mchattie, G. S., 1999, *Adv. Mater.*, **11,** 832.
[7] Meng, X., Natansohn, A., Barretl, C., and Rochon, P., 1996, *Macromolecules*, **29,** 946.
[8] Abe, J., Hasegawa, M., Matsushima, H., Shirai, Y., Nemoto, N., Nagase, Y., and Takamiya, N., 1995, *Macromolecules*, **28,** 2938.
[9] Berg, R. H., Hvilsted, S., and Ramanujam, P. S., 1996, *Nature*, **383,** 505.
[10] Zhou, W., Fu, R., Dai, R., Huang, Z., and Chen, Y., 1994, *J. Chromatogr.*, **659,** 477.
[11] Saito, Y., Jinno, K., Pesek, J. J., Chen, Y. L., Luchr, G., Archer, J., Fetzer, J. C., and Biggs, W. R., 1993, *Chromatographia*, **38,** 295.
[12] Pesek, J. J., Lu, Y., Sioux, A., and Grandperrin, F., 1991, *Chromatographia*, **31,** 147.
[13] Kumar, U., Kato, T., and Fréchet, J. M. J., 1992, *J. Am. chem. Soc.*, **114,** 6630.
[14] Kumar, U., Fréchet, J. M. J., Kato, T., Ujiie, S., and Timura, K., 1992, *Angew. Chem. int. Ed. Engl.*, **31,** 1531.
[15] Van Nunen, J. L. M., Folmer, B. F. B., and Nolte, R. J. M., 1997, *J. Am. chem. Soc.*, **119,** 283.
[16] Kato, T., Ihata, O., Ujiie, S., Tokita, M., and Watanabe, J., 1998, *Macromolecules*, **31,** 3551.
[17] Kawakami, T., and Kato, T., 1998, *Macromolecules*, **31,** 4475.
[18] Stewart, D., and Imrie, C. T., 1997, *Macromolecules*, **30,** 877.
[19] Li, X., Goh, S. H., Lai, Y. H., and Cheng, S. X., 2001, *Liq, Cryst.*, **28,** 1527.
[20] Li, X., Goh, S. H., and Lai, Y. H., 2002, *Liq. Cryst.*, **29,** 675.
[21] Ujiie, S., and Limura, K., 1992, *Macromolecules*, **25,** 3174.
[22] Wright, P. V., 1995, *J. mater. Chem.*, **5,** 1275.
[23] Gohy, J. F., Vanhoorne, P., and Jérôme, R., 1996, *Macromolecules*, **29,** 776.
[24] Percec, V., Johansson, G., Heck, J., Ungar, G., and Batty, S. V., 1993, *J. chem. Soc., Perkin Trans.*, **1,** 1411.
[25] Percec, V., Johansson, G., and Rodenhouse, R., 1992, *Macromolecules*, **25,** 2563.
[26] Bengs, H., Renkel, R., and Ringsdorf, H., 1991, *Makromol. Chem., rapid Commun.*, **12,** 439.
[27] Ringsdorf, H., Wüstefeld, R., Zerta, E., Ebert, M., and Wendorff, J. H., 1989, *Angew. Chem. int. Ed. Engl.*, **28,** 914.
[28] Zhang, B. Y., Guo, S. M., and Shao, B., 1998, *J. appl. Polym. Sci.*, **68,** 1555.
[29] Srikhirin, T., Jr, J. A. M., and Lando, J. B., 1999, *J. polym. Sci. A: polym. Chem.*, **37,** 1057.
[30] Chien-Chang, G. P., 1998, *J. polym. Sci.: polym. Chem.*, **36,** 2849.
[31] Milano, J. C., Robert, J. M., Vernet, J. L., and Gallot, B., 1999, *Macromol. Chem. Phys.*, **200,** 1580.
[32] White, M. S., 1993, *Siloxane Polymer* (Englewood Cliffs: Prentice Hall).
[33] Xu, Z. S., Lemieux, R. P., Natansohn, A., Rochon, P., and Shashidhar, R., 1999, *Liq. Cryst.*, **26,** 351.
[34] Li, X., Goh, S. H., Lai, Y. H., and Wee, A. T. S., 2000, *Polymer*, **41,** 6563.
[35] Velada, J. L., Cesteros, L. C., Meaurio, E., and Katime, I., 1995, *Polymer*, **36,** 2765.
[36] Cesteros, L. C., Velada, J. L., and Katime, I., 1995, *Polymer*, **36,** 3183.
[37] Lee, J. Y., Painter, P. C., and Coleman, M. M., 1988, *Macromolecules*, **21,** 954.
[38] Zhou, X., Goh, S. H., Lee, S. Y., and Tan, K. L., 1997, *Appl. surf. Sci.*, **119,** 60.
[39] Jiang, S. M., Xu, W. Q., Zhao, B., Tian, Y. Q., and Zhao, Y. Y., 2000, *Mater. Sci. Eng. C*, **11,** 85.
[40] Wilson, L. M., 1995, *Liq. Cryst.*, **18,** 381.
[41] Kato, T., Uryu, T., Kaneuchi, F., Jin, C., and Fréchet, J. M. J., 1993, *Liq. Cryst.*, **14,** 1311.
[42] Desiraju, G. R., 1991, *Acc. chem. Res.*, **24,** 290.
[43] Desiraju, G. R., 1996, *Acc. chem. Res.*, **29,** 441.
[44] Davidson, P., 1996, *Prog. polym. Sci.*, **21,** 893.
[45] Mallon, J. J., and Kantor, S. W., 1990, *Macromolecules*, **23,** 1249.
[46] Jeffery, G. A., and Maluszynsk, H., 1986, *J. mol. Struct.*, **147,** 127.